

## Poplar wood-methylol urea composites prepared by *in situ* polymerization. II. Characterization of the mechanism of wood modification by methylol urea

Qian Lang, Zeng Bi, Jun-Wen Pu

Faculty of Material Science and Technology, Beijing Forestry University, Qinghua Eastroad 35, Haidian 100083, Beijing, China  
Correspondence to: J.-W. Pu (E-mail: bjfu4521@126.com)

**ABSTRACT:** A prepolymer was used to prepare wood/prepolymer composites by a pulse-dipping machine. The mechanical properties and dimensional stability were evaluated. The characterization of natural and modified woods was performed by Fourier transform infrared spectroscopy,  $^{13}\text{C}$ -NMR spectroscopy, X-ray photoelectron spectroscopy (XPS), and scanning electron microscopy (SEM) with energy-dispersive X-ray analysis (EDXA). Cross-polarization/magic-angle spinning  $^{13}\text{C}$ -NMR analysis revealed that the *in situ* polymerization between the prepolymer and the hydroxyls in the wood structure took place with the reduction of hydroxyl groups. XPS analysis indicated that the content of carbon decreased, whereas the content of oxygen increased. SEM-EDXA indicated a good dispersion of the modifier in the wood fiber and other vertical cells. © 2015 Wiley Periodicals, Inc. *J. Appl. Polym. Sci.* **2015**, *132*, 42406.

**KEYWORDS:** biomaterials; biopolymers and renewable polymers; crosslinking; mechanical properties; resins

Received 22 May 2014; accepted 22 April 2015

DOI: 10.1002/app.42406

### INTRODUCTION

Wood is one of the oldest and most common renewable materials used in human activities because of its many excellent material properties; these include its good mechanical strength, aesthetic appearance, and easy processing.<sup>1</sup> Despite its excellent engineering properties, it has some serious disadvantages; these include its dimensional instability, low durability, and relatively low mechanical strength, which may prevent wood from replacing materials that are based on unrenovable resources.<sup>2</sup> To overcome these drawbacks, chemical modification is an effective and promising method for improving the properties of wood.<sup>3</sup> Chemical modification provides the means of permanently altering natural wood cell walls by grafting polymers into the wood or by bulking or crosslinking within the wood cell walls.<sup>4</sup> Chemical materials penetrate the cell wall as monomers and polymerize *in situ*. As the cell wall is swollen with polymers, the dimensional stability is enhanced.<sup>5</sup> Generally, esters, isocyanates, acetals, epoxides, phenol, urea, melamine-formaldehyde resins, poly(ethylene glycol), and acetylation have been extensively studied and exploited.<sup>6</sup>

To date, water-soluble, low-molecular-weight resin systems, such as phenol-formaldehyde resin, urea-formaldehyde resin, and melamine-formaldehyde resin, have been the most studied and most successful nonbonding, cell-wall-swelling impregnation processes.<sup>7</sup> These resins belong to a class of thermosets referred

as *amino resins*, which can be obtained as a result of urea condensation with formaldehyde under a wide range of conditions.<sup>8</sup> For example, phenol-formaldehyde resin has a softening effect, such as steam or heat, which plasticizes the wood cell wall.<sup>9</sup> In this softened state, compression applied in the presence of heat allows not only for the deformation of the cell walls without fracturing but also the curing of the resin while the wood is in its compressed and densified form. Therefore, these resins increase dimensional stability by penetrating and swelling the cell wall and forming a rigid crosslinked network upon curing.<sup>2</sup>

In this study, the *in situ* polymerization between a wood modifier and the active groups of wood was investigated further. The mechanical properties of natural and modified wood were evaluated. Moreover, the reaction that occurred during the modification was characterized by Fourier transform infrared (FTIR) spectroscopy, X-ray photoelectron spectroscopy (XPS), cross-polarization/magic-angle spinning (CP/MAS)  $^{13}\text{C}$ -NMR, and scanning electron microscopy (SEM) with energy-dispersive X-ray analysis (EDXA) with the aim of clarifying changes in the chemical structure caused by modification. The spotlight of the whole study was on the mechanism of chemical modification with methylol urea from a chemical perspective. Compared to the previous studies, in this study, we analyzed the mechanism of modification more deeply. Further work should be performed to develop multifunction modifiers, and this part is currently under investigation in our laboratory.

**Table I.** Chemical Reagents for Wood Impregnation

Name	Prepolymer (%)	Urea (%)	Catalyst (%)
A	10	10	2
B	15	10	2
C	20	10	2
D	10	10	2
E	10	15	2
F	10	20	2

## EXPERIMENTAL

### Wood Materials

Wood samples measuring  $25 \times 25 \times 100 \text{ cm}^3$  ( $T \times R \times L$ ) were prepared from the fresh fast-growing poplar (*Populus euramericana* cv. I-214) as described previously.<sup>10</sup>

**Preparation of the Wood Modifier.** The wood modifier was prepared as described previously.<sup>10</sup> Urea, formaldehyde, and ammonia were used for the synthesis of the prepolymer. The synthesis of the prepolymer was carried out in a reaction vessel. Urea (64% w/w), formaldehyde (25% w/w), and ammonia (11% w/w) were added to the reaction vessel. The reaction mixture was stirred and heated to  $40^\circ\text{C}$  for 3 h. Finally, sodium

hydroxide or hydrochloric acid was used to adjust the pH of the prepolymer to 7–8. The functional modifier was obtained with the prepolymer, urea, and catalyst (citric acid). The purity grade of the chemicals was 99%.

**Preparation of the Wood/Prepolymer Composites.** The dimension of wood samples for impregnation was  $20 \times 20 \times 100 \text{ cm}^3$  in length. Natural wood specimens were soaked in a modified solution with a pulse-dipping machine at pressures of 0.7–0.8 MPa for 2 h. The composition of the chemical reagent for wood impregnation is shown in Table I. Then, the impregnated samples were sewn into blocks of about  $3 \times 10 \times 100 \text{ cm}^3$  ( $T \times R \times L$ ) for thermal treatment. Thermal treatment was performed in a drying kiln for 78 h. The drying kiln temperature was increased from room temperature to  $120^\circ\text{C}$  according to an experimental drying schedule.

The reaction between the wood and modifier was a netted site reaction, as depicted in Figure 1. First, the prepolymer, urea, and catalyst (citric acid) were sufficiently mixed before impregnation [Figure 1(a)]. Figure 1(b) shows that the fresh natural wood was full of water. We also observed that the vessels and cell wall of wood were open. Figure 1(c) shows the wood cross section after impregnation, and we observed that the wood modifier was evenly distributed [Figure 1(d)]. The wood modifier was polymerized *in situ* with the wood fibers, forming a

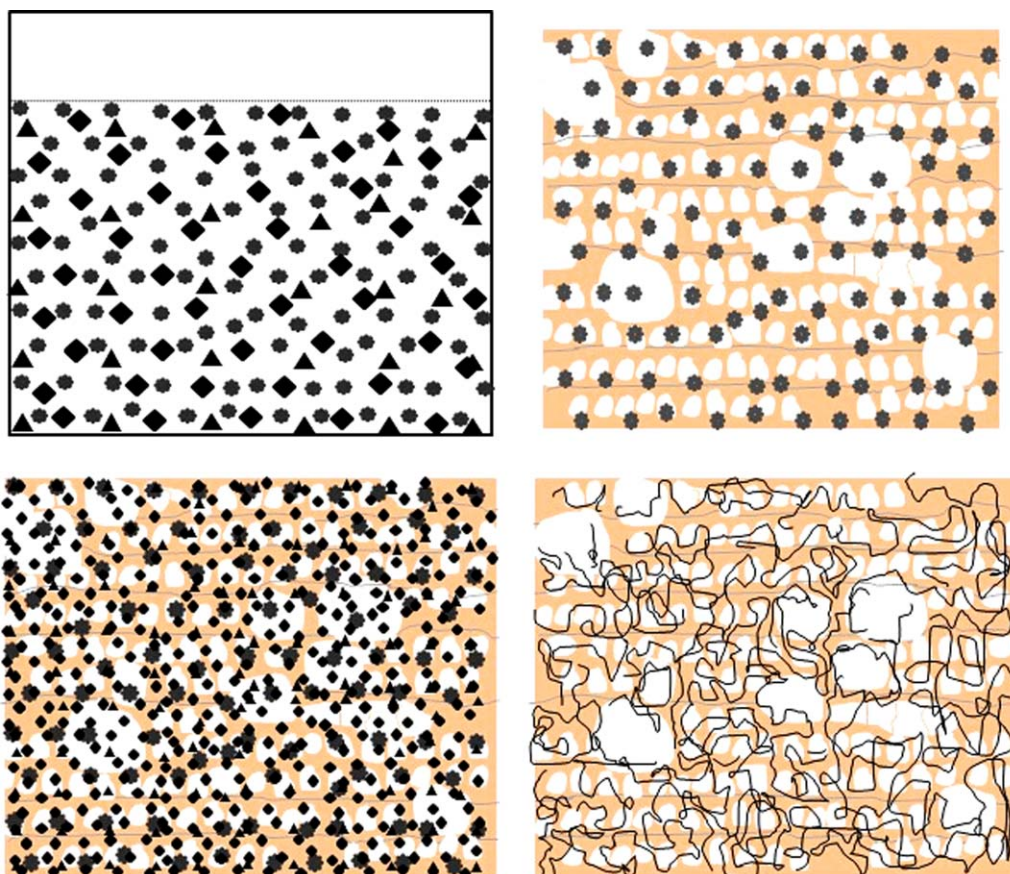


**Figure 1.** Schematic diagram of wood modification [(●) water, (◆) prepolymer, and (▲) urea]: (a) wood modifier, (b) cross section of the natural wood, (c) cross section of the impregnated wood, and (d) cross section of the modified wood after thermal treatment. [Color figure can be viewed in the online issue, which is available at [wileyonlinelibrary.com](http://wileyonlinelibrary.com).]

**Table II.** Mechanical Properties and Dimensional Stability of the Natural and Modified Woods

Name	Basic density (g/cm <sup>3</sup> )	Bending strength (MPa)	Modulus of elasticity in static bending (MPa)	Compressive strength parallel to grain (MPa)	End hardness (N)	Water uptake at 96 h (%)	Swelling (vol %)
Natural wood	0.37	65.20	6546	43.50	2986	118.65	11.30
A	0.47	87.50	8202	55.60	3250	91.83	10.45
B	0.49	106.80	10,720	61.30	4272	88.28	9.88
C	0.57	121.60	10,287	69.80	4932	76.25	9.63
D	0.40	92.10	8295	57.90	3396	110.22	10.26
E	0.51	110.40	9272	62.80	4071	109.38	10.07
F	0.55	120.60	10,020	73.50	4878	85.19	9.52

network and exhibiting higher physical properties and dimensional stability.

**Mechanical Properties and Dimensional Stability.** Ten specimens of natural and modified wood were analyzed with a universal mechanical testing machine (MWW-50). The tests followed Chinese standards GB/T 1933–2009, GB/T 1936.1–2009, GB/T 1936.2–2009, GB/T 1935–2009, GB/T 1941–2009, GB/1934.1–2009, and GB/1934.2–2009 and previous reported work.<sup>11–17</sup> The experiments measuring the free formaldehyde content were done according to Chinese standard GB/18580-2001.<sup>18</sup>

#### Characterization of the Wood/Prepolymer Composites

The FTIR spectra of samples were recorded on a Tensor 27 spectrometer (Bruker, Germany) at a resolution of 64 scans. The transmittance range of the scans was 400 to 4000 cm<sup>-1</sup>.

The solid-state <sup>13</sup>C-NMR spectra of the samples were obtained at 100 MHz with a Bruker AV-III 400M spectrometer (Germany). Acquisition was performed with a cross-polarization pulse sequence. The pulse angle was 60° (8.3 μs), and the relaxation delay was 1.89 s. Approximately 30,000 scans were accumulated for each spectrum.

XPS measurements were performed on an ESCALab250 spectrometer with Al K $\alpha$  radiation as excitation sources. The X-ray source was operated at low power (150 W) to minimize sample damage. The pressure in the analysis chamber was 6.5 × 10<sup>-10</sup> mbar. Survey spectra for each sample over a binding energy

range were 0–1200 eV. The binding energy scale was referenced to the C1s peak at 284.6 eV to compensate for the surface charging effects.

SEM images were obtained by a Hitachi 3400N scanning electron microscope at acceleration voltages of 10 kV and 10 nA. A JSM 5900 energy-dispersive X-ray analyzer was used to investigate the distribution and of C and N in the microstructure of the samples. The samples were sputtered-coated with a thin layer of gold, and the experiment was tested at 15 kV.

## RESULTS AND DISCUSSION

### Mechanical Properties and Dimensional Stability

The average values of the mechanical properties of the natural and modified wood are presented in Table II. As shown in Table II, the mechanical properties of the natural wood were enhanced with increasing contents of prepolymer and urea. The modified wood exhibited a much higher basic density than natural wood. The end hardness of the modified wood increased to 4272 from 2986 N (sample B). Similar to the density and end hardness, the bending strength, compressive strength parallel to the grain, and modulus of elasticity static in bending were increased with increasing contents of the modifier. These results indicate that the prepolymer participated in the *in situ* polymerized reaction to form complicated large molecules. The modifier had the ability to fill the void spaces, and the strong, branched polymer inside the wood enhanced the adhesion and compatibility between the wood fibers and the prepolymer.<sup>19</sup> Moreover,

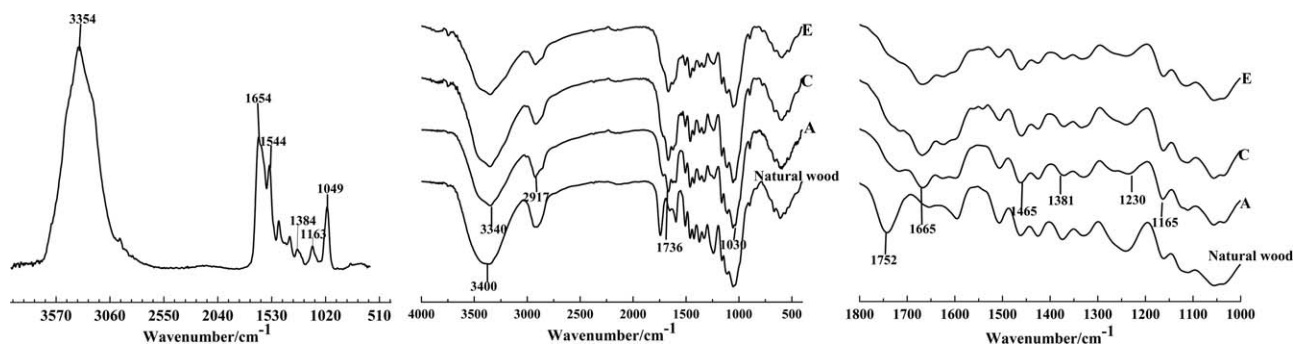


**Figure 2.** FTIR spectra of the natural and modified woods: (a) modifier, (b) natural and modified woods (400–4000 cm<sup>-1</sup>), and (c) modified wood (1000–1800 cm<sup>-1</sup>).

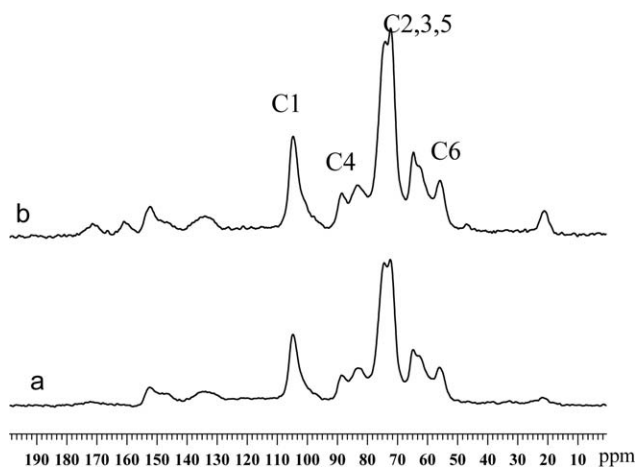


**Figure 3.**  $^{13}\text{C}$ -NMR spectra of wood: (a) natural wood and (b) modified wood.

the degradation of hemicelluloses during the thermal treatment enhanced the mechanical properties of the wood.

The modified wood exhibited better water resistance compared to the natural wood. As is obvious in Table II, all eight types of modifier showed reductions in the water absorption and volu-

metric swelling with increasing amount of prepolymer and urea. The least water uptake decreased from 118.65 to 76.25% (sample C) after modification. The volumetric swelling of wood dropped from 11.30 to 9.52% (sample F). It was reasonable to assume that the prepolymer could polymerize with the wood fiber; this decreased the amount of hydroxyl groups inside wood. The prepolymer not only bulked the cell wall but also interacted with the wood fiber through *in situ* polymerization. The hydrophobic characteristic of the monomers shielded the wood surface and remained in the cell wall and lumen; this resulted in less impregnation of water and moisture.<sup>20</sup> Because of the reaction between the chemical modifier and wood, an improvement in the mechanical properties and reductions in the water absorption and volumetric swelling were noticed. The modified wood was also an environmentally friendly material. The free formaldehyde content of the modified wood was 0.1 mg/100 g.

### FTIR Analysis

The FTIR spectrum of wood modifier is illustrated in Figure 2(a). It was obvious that the modifier contained functional groups. The broad band at  $3354\text{ cm}^{-1}$  was characteristic of  $\text{NH}_2$  stretching vibrations in amino ( $-\text{NH}_2$ ) and imino ( $-\text{NH}$ ) groups and strongly indicated the presence of a large amount of

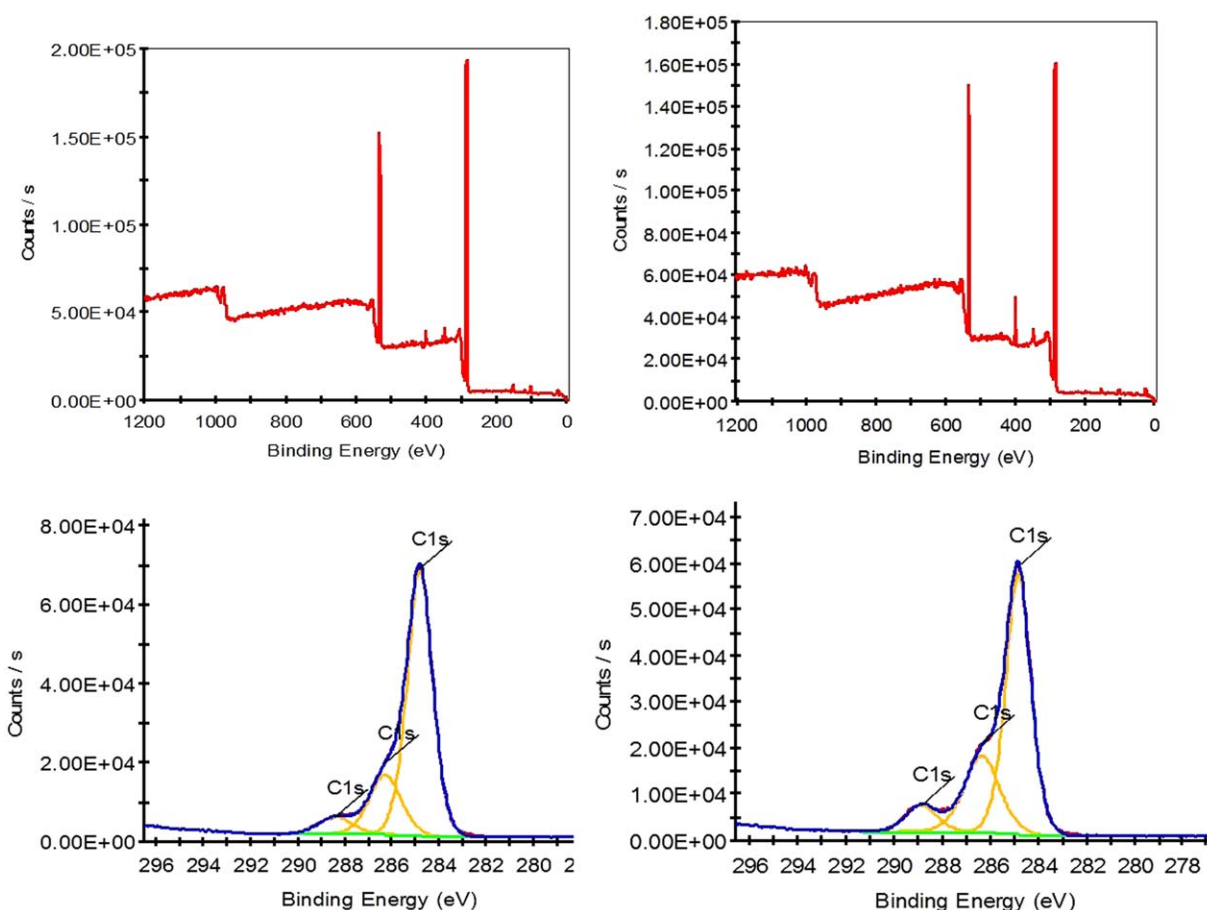


**Figure 4.** XPS spectra of the wood: (a) survey XPS spectrum of the natural wood, (b) survey XPS spectrum of the modified wood, (c) high-resolution  $\text{C}1\text{s}$  XPS spectrum of the natural wood, and (d) high-resolution  $\text{C}1\text{s}$  XPS spectra of the modified wood. [Color figure can be viewed in the online issue, which is available at [www.interscience.wiley.com](http://www.interscience.wiley.com).]

**Table III.** Contents (*n<sub>s</sub>*) of Surface Elements in the Natural and Modified Woods

Sample	<i>n<sub>C</sub></i> (%)	<i>n<sub>O</sub></i> (%)	<i>n<sub>N</sub></i> (%)	<i>n<sub>Si</sub></i> (%)	<i>n<sub>Ca</sub></i> (%)	<i>n<sub>O</sub>/n<sub>C</sub></i> (%)
Natural wood	76.37	18.09	2.42	2.25	0.87	23.67
Modified wood	72.35	21.08	4.81	1.14	0.62	29.14

amino and imino groups in the modifier. The absorption at 3400  $\text{cm}^{-1}$  was assigned to the hydroxyl groups ( $-\text{OH}$ ).  $\text{C}-\text{O}-\text{C}$  asymmetric stretching appeared at 1163  $\text{cm}^{-1}$ . The band at 1752  $\text{cm}^{-1}$  was for  $\text{C}=\text{O}$  ester, that at 1384  $\text{cm}^{-1}$  for  $-\text{C}-\text{CH}_3$ , and that at 1249  $\text{cm}^{-1}$  for  $-\text{C}-\text{O}$  stretching. The band at 1049  $\text{cm}^{-1}$  was attributed to  $\text{C}-\text{O}$  stretching vibrations of methylol in the rings.<sup>21</sup> The absorption at 789–800  $\text{cm}^{-1}$  was associated with  $\text{C}-\text{O}-\text{C}$  stretching vibrations of uron rings, which were assigned to the skeletal vibration of the cyclic structure.<sup>22</sup> The characteristic bands of amide I and II were around 1654 and 1544  $\text{cm}^{-1}$ , respectively.<sup>23</sup> The presence of characteristic bands indicated that the structure of the wood modifier contains various active groups.

The FTIR spectra of the natural and modified woods in the wave-number range from 400 to 4000  $\text{cm}^{-1}$  are shown in Figure 2(b). The peak at 3400  $\text{cm}^{-1}$  was assigned to the stretching vibrations of hydroxyl groups, and the peak position moved to a lower wave number (3340  $\text{cm}^{-1}$ ) as the intensity decreased after modification. All of these observations suggested that a crosslinked bond was formed between the hydroxyl groups of the wood cell walls and the wood modifier. In other words, with the transfer of hydroxyl groups from the wood cell walls to the polymer chains, the broad  $-\text{OH}$  stretching band sharply decreased. Moreover, the absorption bands in the regions of 2917, 1736, and 1030  $\text{cm}^{-1}$  were due to  $\text{C}-\text{H}$  stretching vibrations,  $\text{C}=\text{O}$  stretching vibrations, and  $\text{C}-\text{O}-\text{C}$ , respectively. Furthermore, the intensities of  $-\text{CH}_3$  (2930  $\text{cm}^{-1}$ ) and  $-\text{CH}_2$  (2856  $\text{cm}^{-1}$ ) groups also increased after modification. The changes in these characteristic absorption bands in the modified wood verified that the *in situ* polymerization was successfully conducted.<sup>24</sup>

Figure 2(c) represents the FTIR spectra of the natural and modified woods in the wave-number range from 1000–1800  $\text{cm}^{-1}$ . The formation of chemical bonds between the wood hydroxyl groups and the modifier was evidenced by absorptions at 1752, 1230, and 1381  $\text{cm}^{-1}$ , which were characteristic of the  $\text{C}=\text{O}$ ,  $\text{C}-\text{N}$ , and ( $-\text{C}-\text{CH}_3$ ), respectively, and appeared after modification. An increased intensity at 1165  $\text{cm}^{-1}$  ( $\text{C}-\text{O}$  stretching) indicated the formation of ether bonds. The increased intensity in the 1465  $\text{cm}^{-1}$  ( $\text{CH}_2$  scissoring) band was attributable to an increase in methylene groups. The absorption peak at 1665  $\text{cm}^{-1}$  was amide ( $\text{N}-\text{C}=\text{O}$ ) and

was caused by the bond between the functional groups of  $-\text{NHCH}_2\text{OH}$  (prepolymer) and  $\text{C}=\text{O}$  (wood).

### Solid-State $^{13}\text{C}$ -NMR Analysis

To clarify the complicated relationship between the functional groups and their corresponding chemical shifts in modification, the signal assignments for the CP/MAS  $^{13}\text{C}$ -NMR spectra are presented in Figure 3. Obviously, the dominant pattern of the two spectra was that of the carbohydrates in the region of 50–110 ppm, namely, C-1 (104 ppm) and C-4 (90 ppm, crystal interior cellulose, and 85 ppm, crystal-surface cellulose). The signals at 63 and 65 ppm were assigned to C-6 of the amorphous and crystalline celluloses, respectively. The signals at 73–75 ppm correspond to C-2, C-3, and C-5 of cellulose. The most important chemical shifts were located at 171.43, 134.02, 83.25, 82.40, and 74.44 ppm; this revealed the reactions of the functional groups in modification. The appearance of bands at 135 ppm was typical for  $\text{R}-\text{CH}=\text{O}$  and  $\text{R}-\text{C}=\text{O}$ . More significantly, the *in situ* polymerization clearly appeared to have occurred, as shown by the appearance of the 83.25- and 88.62-ppm bands characteristic of C-4 of amorphous cellulose and crystalline cellulose. The decrease in the signals at 83.25 and 88.62 ppm were interpreted as evidence that the structure of cellulose was not changed. Meanwhile, the etherification in the amorphous region decreased the number of hydroxyl groups in cellulose. The shoulder at 104 ppm on the C-1 cellulose signal belonged to the hemicelluloses. Additionally, the signals of acetate groups and carbonyl groups attached to hemicelluloses resonated at 22 and 172 ppm, respectively. Thermal treatment caused a reduction in the relative intensity of the shoulders at 62, 74, 89, 104, and 172 ppm and suggested some degradation of the hemicelluloses.<sup>25</sup> The decreased intensity of the 74-ppm band indicated that the groups of modifier also reacted at the C-2 position of hemicellulose. The 172-ppm band arose from the carbonyl group of the modified wood and indicated that crosslinking reaction of the hemicellulose by prepolymer occurred mainly at the C-6 position. The lignin was composed of guaiacyl, syringyl, and *p*-hydroxyphenyl.<sup>26</sup> The lignin methoxyl groups gave a signal at 58 ppm. The resonances in the chemical shift range of 119–122 ppm were assigned to C-2 and C-6 of the syringyl units. Additionally, the signal at 135 ppm was assigned to C-1/C-4 of the syringyl units and C-1 of the guaiacyl units. In the combined results obtained from the CP/

**Table IV.** High-Resolution C1s XPS Spectra of the Natural and Modified Woods

Sample	Peak position $E_B$ (eV)			Separation $E_B$ (eV)			Area (%)		
Natural wood	284.73	287.05	288.41	1.35	1.67	1.81	72.74	20.75	6.51
Modified wood	284.89	287.42	288.79	1.24	1.74	1.62	64.45	27.08	8.47

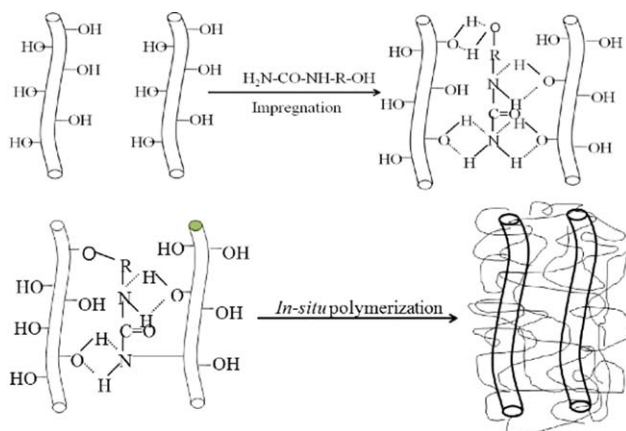


**Figure 5.** Schematic representation of *in situ* polymerization. [Color figure can be viewed in the online issue, which is available at wileyonlinelibrary.com.]

MAS spectra and FTIR spectra, the band at  $1750\text{ cm}^{-1}$  for  $\text{C}=\text{O}$  in modified wood decreased after modification; this was consistent with the observation that the absorption band at 172

ppm ( $\text{C}=\text{O}$ ) in the  $^{13}\text{C}$ -NMR spectrum of modified wood was also absent. These results suggest that the structure of xylan was changed and that the *in situ* polymerization occurred between the carbonyl group of cellulose and the modifier.

#### XPS Analysis

Figure 4(a,b) shows the typical XPS survey spectra of the natural and modified woods. Table III lists the experimental atomic compositions as determined from the XPS spectral analysis and the calculated oxygen-to-carbon (O/C) atomic ratio for the natural and modified woods. According to the XPS survey spectra, the natural and modified wood consisted mainly of C and O; this is characteristic of cellulose. The natural wood was expected to show a relative oxygen-to-carbon ratio of 24.11 (C, 76.37%, and O, 18.09%). However, the O/C atomic ratio of the modified wood was much higher than that of the natural one. Table III shows some decrease in the percentage of carbon atoms and some increase in the percentage of oxygen atoms after modification. The increase in O/C was due to the *in situ* polymerization and hydrolysis reactions that took place during modification. The percentage of nitrogen increased to 4.81%; this was

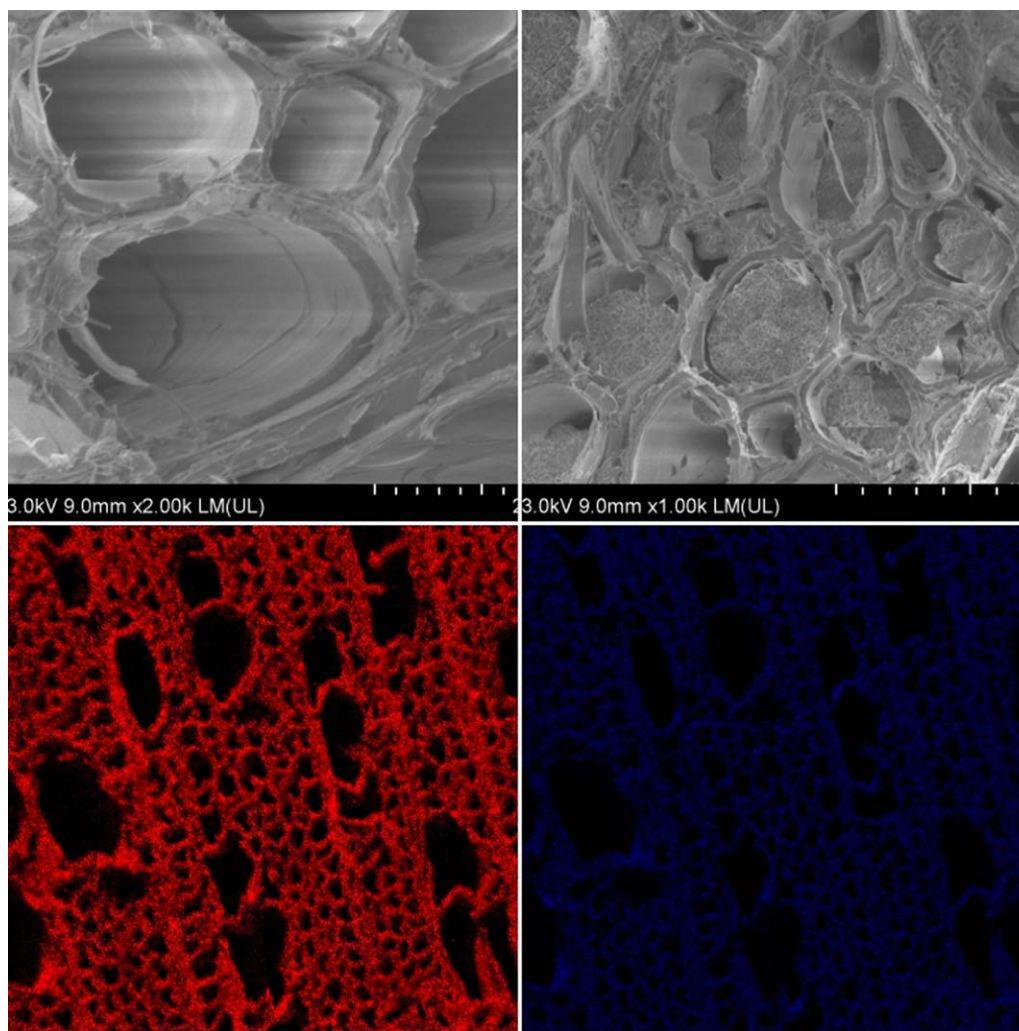


**Figure 6.** SEM-EDXA analysis of the natural and modified woods: (a) transection of the natural wood, (b) transection of the modified wood, (c) distribution of C, and (d) distribution of O. [Color figure can be viewed in the online issue, which is available at wileyonlinelibrary.com.]

attributable to the *in situ* polymerization and the urea of the modifier.

Figure 4(c,d) shows the C1 high-resolution spectra of the natural and modified woods. From the deconvolution of the natural wood curve and Table IV, we observed that the C1 peak could be fitted into three peaks at 284.73, 287.05, and 288.41 eV, which were attributed to C1, C2, and C3. C1 corresponds to a carbon atom bound only to other carbon atoms and/or hydrogen atoms (C—H or C—C); they were mainly from lignin and extractives,<sup>27</sup> and the relative content was 72.74%. C2 is from carbon atoms bonded to a single oxygen atom (C—O); the relative content was 20.75%. C3 is from carbon atoms bonded to two noncarbonyl oxygen atoms or to a single carbonyl oxygen atom (O—C—O, C=O); the relative content was 6.51%. After modification, the relative content of C1 was low at 64.45%; however, the relative content of C2 and C3 increased to 27.08 and 8.47%. The decrease in the C1 carbon concentration after modification indicated that the surface of the modified wood was oxidized, and oxygen-containing groups, such as —C—O—, —C=O, and —O—C=O bond were generated (from cellulose decomposition and/or the presence of impurities like lignin and fatty acids). This was accompanied by a significant increase in the concentration of C3.<sup>28</sup> Hence, the content of —C—C— and —C—H bond decreased.<sup>29</sup> The concentration of C2 increased as a result of reaction with wood modifier; this confirmed that the chemical reaction occurred between the functional groups of —NHCH<sub>2</sub>OH from the prepolymer groups and the wood carboxyl C=O. These results were consistent with the variation observed by FTIR spectroscopy for the bands that were assigned to C—O and C=O and/or O—C—O stretching vibrations. The chemical reaction mechanism for *in situ* polymerization involving two steps is shown in Figure 5; it shows the major chemical connection structure between the wood fiber and functional groups of the wood modifier.<sup>10</sup>

#### SEM–EDXA Analysis

To verify how the wood modifier existed in the inner wood structure, SEM pictures of the natural and modified woods were recorded. For the natural wood, the cell wall and vessel exhibited a highly voided structure [Figure 6(a)]. Moreover, empty cell walls, pits, and parenchyma were observed in the micrographs. After modification, the modifier was homogeneously dispersed in the cell wall [Figure 6(b)]. The EDXA micrographs [Figure 6(c,d)] presented the distribution of carbon and nitrogen in the cell wall and intercellular space. The statistics manifested that the content of carbon was 59.87 mol % and the content of oxygen was 30.12 mol %. The good dispersion of the modifier in the wood fiber and other vertical cells was ascribed to the chemical bonds between the wood and prepolymer. In addition, the interfacial adhesion of the wood modifier contributed to an improvement in the physicochemical properties of the wood.

#### CONCLUSIONS

An effective *in situ* polymerization on poplar wood was carried out by functional modifiers. We found that the physical properties and dimensional stability of natural wood were improved

after modification. FTIR, XPS, and <sup>13</sup>C-NMR analysis clarified the complicated relationship between the functional groups of the modifier and the wood fiber. After modification, the absorption of active groups such as C—O and C=O and/or C—O—C were assigned to the bonds between the wood and functional groups of the wood modifier. Moreover, the chemical shifts in modification, especially the C=O group, clarified the relationship between the functional groups and the wood cells, as shown by <sup>13</sup>C-NMR. XPS analysis showed that the surface of the modified wood was oxidized, and oxygen-containing groups, such as —C—O—, —C=O, and —O—C=O bond, were generated. Finally, SEM–EDXA provided evidence that the wood modifier was distributed in the wood fiber and other vertical cells. Compared to previous studies, methylol urea was used to modify the poplar wood by *in situ* polymerization. The mechanical properties and dimensional stability of the wood–methyl urea composites improved remarkably. FTIR analysis suggested that the methylol urea polymerized with the active groups of the wood cell wall. X-ray diffraction (XRD) showed that the crystallinity of wood increased after modification. However, the location of the peaks did not change; this indicated that the ordered structure of the crystalline region on the remaining cellulose was not disrupted during modification. This study emphasized the mechanism of chemical modification with methylol urea. Compared to methylol urea, the melamine–urea–formaldehyde prepolymer showed better water-resistance behavior. Meanwhile, the modified wood with the melamine–urea–formaldehyde prepolymer demonstrated better dynamic mechanical properties.

#### ACKNOWLEDGMENTS

This research was supported by the Forestry Public Industry Foundation (contract grant number 201204702-B2, “Research on Key Techniques for Fast-Growing Wood for Furniture”). The authors are grateful for the support of the China Scholarship Council.

#### REFERENCES

1. Moreau, C.; Belgacem, M. N.; Gandini, A. *Top. Catal.* **2004**, *27*, 11.
2. Shams, M. I.; Kagemori, N.; Yano, H. *J. Wood Sci.* **2004**, *50*, 337.
3. Noël, M.; Mougél, E.; Fredon, M.; Masson, D.; Masson, E. *Bioresour. Technol.* **2009**, *100*, 4717.
4. Xie, Y. J.; Xiao, Z. F.; Grüneberg, T.; Militz, H.; Hill, C. A. S.; Steuernagel, L.; Mai, C. *Compos. Sci. Technol.* **2010**, *70*, 2003.
5. Yun, S. Y.; John, R.; Hwang, B. *Polymers* **2012**, *4*, 913.
6. Gabrielli, C. P.; Kamke, F. A. *Wood Sci. Technol.* **2010**, *44*, 95.
7. Guillaume, T.; Bernard, B.; Bruno, A. *Prog. Polym. Sci.* **2011**, *36*, 191.
8. Hisham, A. E.; Abd-Allah, B. M.; Nadia, H. E. *J. Appl. Polym. Sci.* **2009**, *114*, 1348.

9. Hill, C. *Wood Modification: Chemical, Thermal and Other Processes*; Wiley: Chichester, England, **2006**.
10. Lang, Q.; She, Y.; Chen, H. Y.; Pu, J. W. *J. Appl. Polym. Sci.* **2013**, *130*, 933.
11. Chinese standard. GB/T 1933-2009. Method for determination of the density of wood.
12. Chinese standard. GB/T 1936.1-2009. Method of testing in bending strength of wood.
13. Chinese standard. GB/T 1936.2-2009. Method for determination of the modulus of elasticity in static bending of wood.
14. Chinese standard. GB/T 1935-2009. Method of testing in compressive strength parallel to grain of wood.
15. Chinese standard. GB/T 1941-2009. Method of testing in hardness of wood.
16. Chinese standard. GB/1934.1-2009. Method for determination of the water absorption of wood.
17. Chinese standard. GB/1934.2-2009. Method for determination of the swelling of wood.
18. Chinese standard GB/18580-2001. The indoor decorating and refurbishing material-limit of formaldehyde emission of wood-based panels and finishing products.
19. Wan, Y. Z.; Luo, H. L.; Liang, F. H. H.; Huang, Y.; Li, X. L. *Compos. Sci. Technol.* **2007**, *69*, 1212.
20. Islam, M. N.; Rahman, M. R.; Haque, M. M.; Huque, M. M. *Compos. A* **2010**, *41*, 192.
21. Dessipri, E.; Minopoulou, E.; Chryssikos, G. D.; Gionis, V.; Paipetis, A.; Panayiotou, C. *Eur. Polym. J.* **2003**, *39*, 1533.
22. Schranzer, F. C.; Buhner, H. G. Investigation the curing of amino resins with TGS-MS and TGA-FT-IR; Mettler Toledo: **2001**; Vol. 2, p. 13.
23. Liu, Y. Q.; Tian, Y.; Zhao, G. Z.; Sun, Y. Y.; Zhu, F. Z.; Cao, Y. *J. Polym. Res.* **2008**, *15*, 501.
24. Matuana, S. J.; Stark, N. M. *Polym. Degrad. Stab.* **2011**, *96*, 97.
25. Yuan, T. Q.; Sun, S. N.; Xu, F.; Sun, R. C. *Bioresour. Technol.* **2011**, *102*, 4590.
26. Tserkia, V.; Zafeiropoulos, N. E.; Simonb, F.; Panayiotou, C. *Compos. A* **2005**, *36*, 1110.
27. Popescu, C. M.; Tibirna, C. M.; Vasile, C. *Appl. Surf. Sci.* **2009**, *256*, 1355.
28. Sahin, H. T. *Appl. Surf. Sci.* **2007**, *253*, 4367.
29. Liu, Y.; Tao, Y.; Lv, X. Y.; Zhang, Y. H.; Di, M. W. *Appl. Surf. Sci.* **2010**, *257*, 1112.